Fixed-bed adsorption of methylene blue by rice husk ash and rice husk/CoFe$_2$O$_4$ nanocomposite

Kang-Kang Yan[a], Jiao Huang[b], Xue-Gang Chen[a,c], Shu-Ting Liu[a], Ao-Bo Zhang[a], Ying Ye[a], Mei Li[a], Xiaosheng Ji[a],*

[a]*Ocean College, Zhejiang University, Hangzhou 310058, P.R. China, Tel. +86 15864736135; email: yankangkang.1989@163.com (K.-K. Yan), Tel. +86 571 88206655; email: chenxg83@gmail.com (X.-G. Chen), Tel. +86 15067189298; email: liushuting@zju.edu.cn (S.-T. Liu), Tel. +86 13567109727; email: 1988aobo@163.com (A.-B. Zhang), Tel. +86 571 88208825; email: gsyeying@zju.edu.cn (Y. Ye), Tel. +86 13282038128; email: 21334021@zju.edu.cn (M. Li), Tel. +86 571 88981966; Fax: +86 571 88208891; email: jixiaoshen@hotmail.com (X. Ji)*
[b]*YueQing Food Testing Center for Quality and Safety, YueQing 325600, P.R. China, Tel. +86 13758246689; email: geliuqin@zju.edu.cn*
[c]*State Key Laboratory of Satellite Ocean Environment Dynamics, Second Institute of Oceanography, State Oceanic Administration, Hangzhou 310012, P.R. China*

ABSTRACT

Rice husk ash (RHA) is a promising low-cost adsorbent. Meanwhile, the magnetic and catalytic capabilities of ferrite nanoparticles make it efficient for water purification. In this study, we prepared RHA and rice husk/CoFe$_2$O$_4$ composite (RHC) and studied their methylene blue (MB) adsorption capacities in fixed-bed columns. The column regeneration was also investigated. Both RHA and RHC are amorphous materials with Brunauer, Emmet and Teller (BET) surface area of >180 m^2 g^{-1} and mesopore volume of >0.1 cm^3 g^{-1}. The CoFe$_2$O$_4$ nanoparticles are mainly located on the inner surface of RHC, which significantly increased the mesopore volume and average pore size but decreased the BET surface area and micropore volume. The adsorption ability of RHC was investigated in a fixed-bed column, with RHA as control. The effects of column parameters including bed height, flow rate, and inlet MB concentration on breakthrough curves were studied. The mathematical models, such as bed-depth service time (BDST), Thomas, and Yoon–Nelson models were applied to predict the breakthrough curves. It was found that BDST model fitted the breakthrough curves best. Results showed that the breakthrough time of RHC is more than two times than that of RHA, which may be attributed to the catalytic performance of CoFe$_2$O$_4$ nanoparticles. The exhausted RHA and RHC were retreated by three methods and eluted of the column with ethanol caused the highest regeneration efficiency. In addition, fixed-bed tests of RHA and RHC on real dye wastewater demonstrated that these adsorbents have good practical value and application prospect.

Keywords: Rice hull; Methylene blue; Adsorption; Fixed-bed column; Ferrite

---

*Corresponding author.

1. Introduction

Environmental contamination caused by dyes has gained global focus. Dyes present low toxicity to mammals or aquatic organisms and have long been used in the fields of dyeing, paper and pulp, textiles, plastics, leather, cosmetics, and so on [1,2]. However, it is a visible pollutant and the presence of even a trace amount of coloring substance makes it undesirable [3]. There are many technologies to purify the dyeing wastewater, such as photocatalytic degradation [4], oxidation process [5], electrochemical technology [6], membrane filtration [7], ion-exchange process [8], biological treatment [9], and adsorption [10]. Among these technologies, adsorption has been proven to be an effective process for dye removal [11]. It has advantages over other techniques in terms of low initial cost, flexibility and simplicity of design, ease of operation, and so on [12]. Activated carbon (AC) is one of the most widely used adsorbent in the water treatment [13]. AC is a widely used sorbent for dyes removal; however, the widespread use of AC is restricted by its high cost, leading to the researches on alternative non-conventional and low-cost adsorbents [14]. Agricultural products are available in large quantities around the world and rice husk is the byproduct during the paddy process in rice milling industry. The generated rice husk is in large quantities, which pose a serious problem to environment and the applicability of rice husk as foodstuff for cattle or as power source is limited [15,16]. Due to its abundant production, low cost, and high contents of silica and carbon, it is a potential low-cost biosorbent with efficient adsorption capacity [17,18]. Many studies have investigated the use of rice husk as biosorbent with high adsorptive capacity, such as heavy metal removing [19], dye wastewater purification [20,21], toxic substances removal from landfill leachate [22], and oil compounds treatment [23].

Ferrites, with general formula of AFe_2O_4 (A = Mn, Zn, Ni, Co, Fe, etc.), are magnetic materials with cubic spinel structure. Ferrite catalysts have been employed in various reactions, such as Knoevenagel reaction [24], Fenton catalyst reaction [25], and so on [26]. Nano-sized ferrite particles are also potential wastewater-treating agents [27,28]. The magnetic and catalytic abilities of ferrite make it potential to enhance the treating efficiency and also make the adsorbents recyclable [29]. Dong et al. [30] found that $CoFe_2O_4$ nanosphere consisting of nanoparticles display high adsorption performance on organic dyes. Ai et al. [31] combined the AC with $CoFe_2O_4$ to create a composite which could be used as a promising and effective adsorbent for the removal of malachite green from water.

In our previous work, we have studied the thermal destruction of rice husk in air and nitrogen and the adsorption properties of rice husk ash (RHA) [32,33]. The rice husk/ferrite composites were synthesized and characterized. In addition, synthesized rice husk/ferrite nanocomposites were used for methylene blue (MB) removal in batch mode [29,34]. But there are few studies about the MB adsorption behavior of rice husk/$CoFe_2O_4$ composite (RHC) in fixed-bed column method. Batch adsorption experiments are usually used in laboratory to study the adsorption kinetics, equilibrium, and thermodynamics, while in industries the fixed-bed column is more commonly used. In this study, we prepared RHA pyrolyzed from rice husk and RHCs, and studied their MB adsorption properties in fixed-bed column at laboratory scale. The effects of bed height, initial MB concentration, and flow rate on column adsorption were studied in detail. Some common theoretical models were applied to fit the breakthrough curves. The regenerating and reuse of the adsorbents were studied in various adsorption–regeneration cycles. In order to test the feasibility of RHA and RHC for real practical use, we used practical dye wastewater to conduct the fixed-bed adsorption experiments.

2. Materials and methods

2.1. Materials

Rice husk was obtained from Hangzhou, Zhejiang Province. MB, a cationic dye, was supplied by Aladdin Industrial Corporation (Shanghai, China). HCl (36–38%), ethanol (C_2H_5OH, 99.7%), $Co(NO_3)_2 \cdot 6H_2O$, and $Fe(NO_3)_3 \cdot 9H_2O$ were purchased from Sinopharm Chemical Reagent Co. Ltd. (Shanghai, China). All reagents were used without further purification and deionized water was used throughout this study.

2.2. Preparation of the samples

In a typical procedure, two solutions: 100 mL $Co(NO_3)_2$ (0.25 mol L^{-1}) solution and 100 mL $Fe(NO_3)_3$ (0.5 mol L^{-1}) solution were mixed with 100 g rice husk and the mixture was vigorously stirred for 30 min. The mixture was placed in a temperature-controlled oven at 393 K for 2 h. Then, the mixture was transferred into a muffle furnace and heated at 1,023 K for 3 h without air. After cooling to room temperature, RHC nanocomposite was obtained. For comparison, rice husk was directly calcined at 1,023 K for 3 h with the absence of air to obtain RHA. The heating rates were 10 K min^{-1} for all treatments.

2.3. Characterizations

The crystallinity and phases of RHC and RHA were carried on a D/max 2550 X-ray diffractometer (Rigaku, Japan) with Cu Kα radiation at scan rate of $0.02° s^{-1}$. The surface morphologies of the samples were evaluated by a 650 FEG Field 108 Emission Scanning Electronic Microscope (Quanta, USA) at accelerating voltage of 10–20 kV. The specific surface area and pore characteristics of the samples were measured by nitrogen adsorption and desorption at 77 K using an AUTOSORB-1-C surface area and pore analyzer. The pore volume and pore size distribution of RHA and RHC were estimated by the Barrett–Joyner–Halenda (BJH) method.

2.4. Adsorption studies by fixed-bed column

Fixed-bed column adsorption experiments were conducted in glass columns with 8 mm in diameter and 300 mm in length, MB solution was pumped in a down flow mode through the fixed-bed with certain amount of samples, using a multi-channel peristaltic pump at specified flow rates. The output samples were collected at regular interval and then were analyzed to yield the output MB concentrations (C_t). The breakthrough time was determined as time t when $C_t/C_0 = 0.05$. The operation temperature for all experiments was maintained at 293 K. The MB concentrations were measured at 664 nm (λ_{max}), using a TU-2550 UV–vis spectrophotometer (Purkinje General Instrument Co. Ltd., Beijing).

2.5. Regeneration of the column

In order to reuse the adsorbents and regenerate the saturated column, the exhausted adsorbents were retreated by three methods: the exhausted adsorbents in the column were eluted with $0.1 mol L^{-1}$ HCl solution, ethanol (99.7%), or heated in a microwave oven. The flow rate of the eluting process was maintained at $2 min L^{-1}$ until the outlet of the column became colorless, the microwave oven power of 700 W and the frequency of 2,450 MHz were selected. The regeneration progress was carried out after the adsorption progress reached the breakthrough point of the curve. The cycle of adsorption–regeneration were repeated three times in the same way. The regeneration efficiency (RE) was calculated using Eq. (1).

$$RE = \frac{q_r}{q_0} \times 100 \tag{1}$$

2.6. Practical wastewater treatment

The real dye wastewater was collected from a dying industry situated at Shaoxing, China. The wastewater contains various electrolytes such as Na_2S ($355 mg kg^{-1}$), $NaCO_3$ ($420 mg kg^{-1}$), NaCl ($350 mg kg^{-1}$), and other auxiliaries. The industrial wastewater sample was spiked with MB to reach the concentration of $20 mg L^{-1}$ and the pH of the solution was 8.6. The wastewater was treated in the fixed-bed column; the flow rate and bed height were kept at $10 mL min^{-1}$ and 200 mm, respectively.

3. Results and discussion

3.1. Characterization of samples

Both RHA and RHC were characterized by X-ray diffraction (XRD), scanning electronic microscope (SEM), and Brunauer, Emmet and Teller (BET) to show their physico-chemical characteristics. Fig. 1 (left) shows the XRD patterns of RHA and RHC. Both samples exhibit a broad peak at around $2\theta = 22°$, which can be attributed to the amorphous silica pyrolyzed from rice husk [33]. Typical crystal faces of $CoFe_2O_4$ (JCPDF# 22-1086) (2 2 0), (3 1 1), and (4 0 0) can be identified from the diffraction peaks of RHC, which proved the successful preparation of RHC.

The corresponding SEM images of RHA and RHC are consistent with XRD analyses that both samples are amorphous materials. The micro-morphology of RHA shows that many protuberances from raw rice hull and many particles distribute on the outer surface, while the inner surface is relatively smooth, which attributed to the retention of carbon that originated from organic matters in the rice husk [29,33]. The outer surface of RHC is similar to that of RHA with many protuberances. The inner surface, however, is filled with homogenized $CoFe_2O_4$ nanoparticles with diameter of about 240 nm. It is suggested that the cobalt ferrite particles will be preferentially synthesized on the inner surface of rice husk, which may be attributed to the relatively hydrophobic nature for the outer surface of rice husk [29].

Fig. 2 and Table 1 show the derived BET surface area, pore volumes, pore size distributions of RHC and RHA. Both RHA and RHC show similar mesopore distributions with maximum mesopore volume of about 4 nm, due to the restriction of silica framework in rice husk [33]. However, because ferrite nanoparticles grew along the silica framework and consequently created more mesopores, the mesopore volume and average pore size of RHC are much
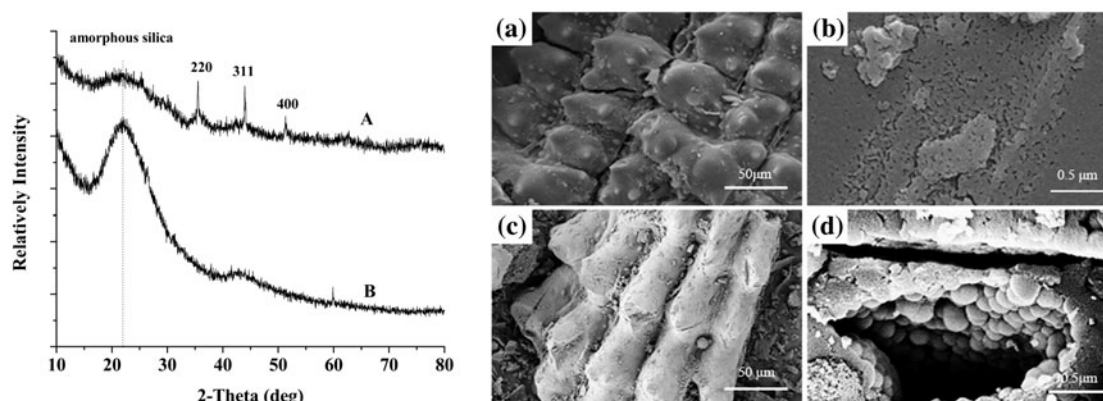
Fig. 1. (Left) XRD patterns of (A) RHC and (B) RHA; (right) SEM images of ((a) and (b)) RHA and ((c) and (d)) RHC.
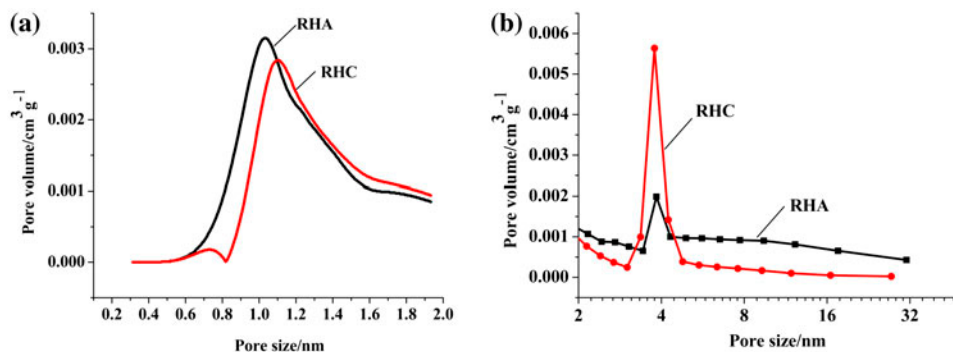
Fig. 2. (a) Micropore and (b) mesopore size distributions of RHA and RHC samples.

Table 1
BET surface area and pore characteristics of RHA and RHC

Samples	BET surface area ($m^2\,g^{-1}$)	Mesopore volume ($cm^3\,g^{-1}$)	Micropore volume ($cm^3\,g^{-1}$)	Average pore size (nm)
RHC	194.7	0.186	0.088	4.90
RHA	309.0	0.118	0.147	2.88

higher than that of RHA. In addition, the ferrite nanoparticles will fill up the existing micropores, the BET surface area and micropore volume of RHC are significantly lower than that of RHA as a result. Because MB molecules can only enter mesopores [32], the mesopore volume is a key factor in determining the MB adsorption capacity of adsorbents.

3.2. Fixed-bed adsorption of MB

3.2.1. Effect of bed heights on breakthrough curves

The effects of bed height on the adsorption performance of RHC and RHA were investigated over a range from 100 to 267 mm. The breakthrough times at different bed heights are shown in Table 2. As expected, increase in bed height will significantly enhance the breakthrough time, because the amount of adsorbent and binding sites are increased consequently. It is observed that the slopes of the breakthrough curves were roughly similar. However, with the increasing of bed heights, the slopes decreased slightly. At the same concentration and flow rate, the increase of bed column length results in a broadened mass transfer zone. The mesopore and surface area are essential on the MB adsorption. Table 1 and Fig. 2 show that RHC presents more than 1.8 times mesopore volume in 3.776–3.837 nm but 40.0% surface area than that of RHA. It is also found that the RHC column exhibits more than three times service times than

Table 2
Column data and parameters obtained at different operation conditions

| | Fixed-bed parameters | | | | | |
| | V_b (mL) | | t_b (min) | | q_0 (mg g^{-1}) | |
Operation conditions	RHA	RHC	RHA	RHC	RHA	RHC
Bed height* (mm)						
100	60.3	226.6	6.03	22.66	6.09	11.73
133	84.1	558.9	8.41	55.89	7.83	15.41
167	142.6	737.7	14.26	73.77	8.00	14.64
200	152.8	1,022	15.28	102.2	7.31	16.26
267	307.2	1,543	30.72	154.3	6.14	15.92
Flow rates (mL min^{-1})						
2.5	1,401	1,455	560.5	581.7	13.73	14.27
5.0	853.5	1,064	170.7	212.8	10.09	12.8
7.5	555.6	493.1	74.08	98.62	10.89	11.72
10	657.4	602.0	65.74	60.20	10.75	10.67
15	255.3	315.9	17.02	21.06	5.64	6.49
20	303.2	302.4	15.16	15.12	5.80	5.75
Inlet MB concentrations (mg L^{-1})						
10	675.5	1,784	67.55	178.4	8.62	12.98
20	657.4	602.0	65.74	60.20	10.75	10.67
50	127.0	408.3	12.70	40.83	12.95	9.18
100	58.4	214.8	5.84	21.48	2.6	10.73

*The data of different bed heights at operation conditions was obtained from the second batch of synthetized samples, which showed some difference from others.

that of RHA, which is disproportionate to the ratios of mesopore size and surface area between RHC and RHA. It is attributed to the fact that the $CoFe_2O_4$ nanoparticles in RHC will catalytically remove MB molecules from aqueous system. It can be verified by our previous work that we investigated the MB removal by RHC for adsorption and degrading organic compounds in the organic wastewater treatment [34]. The catalytic performance of ferrites was also studied in other works [35,36]. According to the

results of our data, the catalytic performance of $CoFe_2O_4$ was certified and the use of rice husk/$CoFe_2O_4$ in fixed-bed is applicable (Fig. 3).

3.2.2. Effect of volumetric flow rate

The effect of the volumetric flow rate on the MB adsorption was studied at 2.5, 5, 7.5, 10, 15, 20 mL min^{-1}. The breakthrough curves are showed in
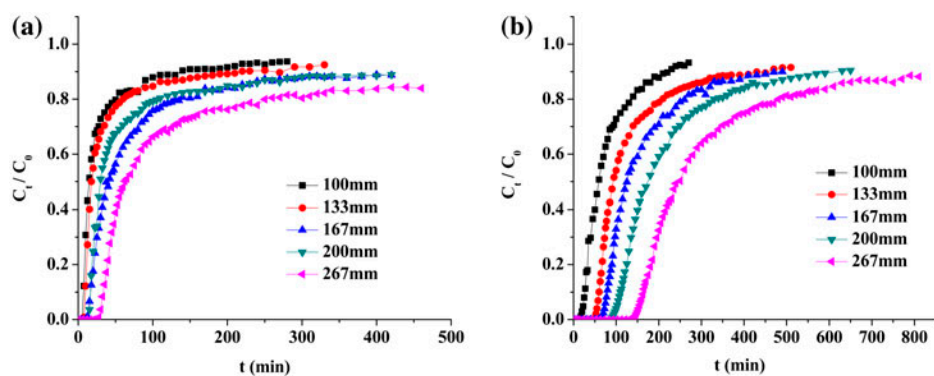
Fig. 3. Breakthrough curves of MB removal by (a) RHA and (b) RHC at different bed height from 100 to 267 mm (flow rate: 10 mL min^{-1}, initial MB concentration: 20 mg L^{-1}).

Fig. 4 and the breakthrough times are shown in Table 2. It is clear that in both cases breakthrough times increase significantly with the decrease of flow rate. When at a low rate, MB molecules have longer time contacting with adsorbents and higher removal efficiency was achieved. In addition, higher contact time in the fixed-bed will increase the possibility of MB molecules diffusing through the internal boundary layer around the adsorbent, which in turn will increase the efficiency of MB adsorption. The results obtained were similar to those reported by other works [37,38]. In both cases, the increase of flow rate will elevate the slopes of the curves, which indicates a decrease in the mass transfer resistance of the progress.

3.2.3. Effect of inlet MB concentration on breakthrough curve

The effect of inlet MB concentration was investigated at 10, 20, 50, 100 mg L^{-1}. The breakthrough curves are plotted in Fig. 5 and the breakthrough times are shown in Table 2. It was illustrated from Fig. 5 and Table 2 that in both cases, breakthrough times decrease with increasing MB concentration. In addition, with the increase of inlet MB concentration, the slopes of the curves become higher, which indicates a faster mass transport. With the same inlet concentration, the breakthrough times achieved by RHC were longer than that of RHA. It is attributed to the catalytic removal of $CoFe_2O_4$ for MB and the catalytic performance of $CoFe_2O_4$ was certified.

3.3. Modeling

3.3.1. Bohart–Adams and bed-depth service time model

The Bohart–Adams model was developed by Bohart and Adams in 1920 [39]. This model was initially applied to a gas–solid system, nowadays it is used for the quantitative description of other types of adsorption systems. This model describes the relationship between C_t/C_0 and t in a fixed-bed system and it assumes that the forces like intra-particular diffusion and external mass transfer resistance are negligible. Therefore, the adsorption rate is proportional to the residual capacity of the solid and the concentration of the adsorbents.
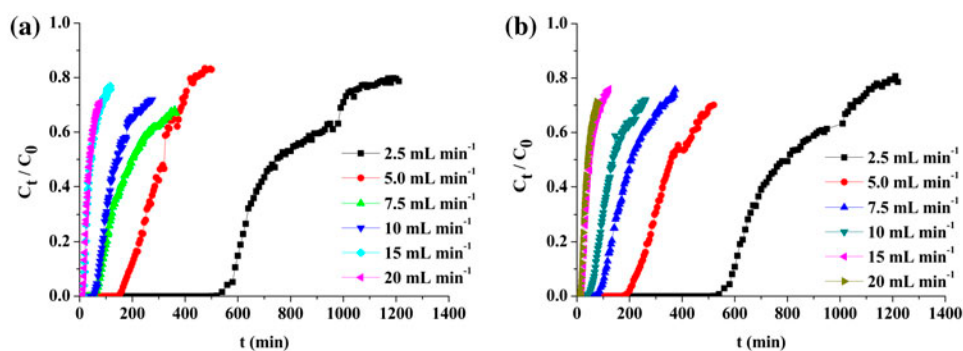
Fig. 4. Breakthrough curves of MB removal by (a) RHA and (b) RHC on different flow rates from 2.5 to 20 mL min^{-1} (bed height: 200 mm, initial MB concentration: 20 mg L^{-1}).
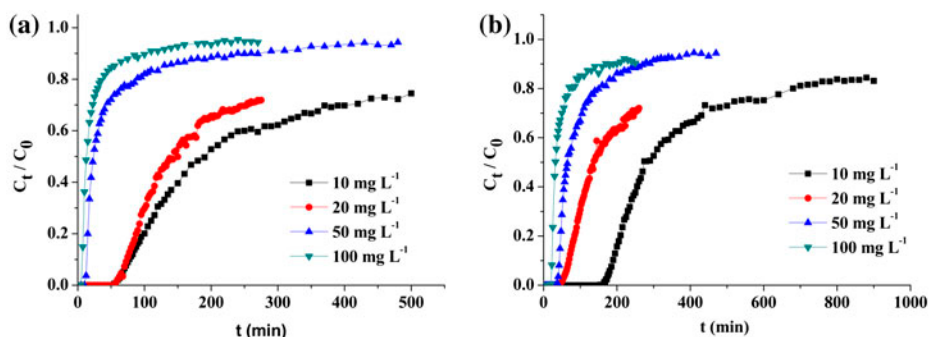
Fig. 5. Breakthrough curves of MB removal by (a) RHA and (b) RHC on different inlet MB concentrations (bed height: 200 mm, flow rate: 10 mL min^{-1}).

This model is used to describe the initial part of the breakthrough curve. Hutchins linearized the Bohart–Adams equation and presented the bed-depth service time (BDST) model which made a correlation between the service time and the fixed-bed height:

$$t = \frac{N_0}{C_0 U} Z - \frac{1}{C_0 k_{AB}} \ln\left(\frac{C_0}{C_b} - 1\right) \qquad (2)$$

Eq. (1) enables the service time (t) of an adsorption bed to be determined by a specified bed depth (Z) of adsorbent. t and Z are correlated with initial MB concentration (C_0), solution flow rate (U), and the adsorption capacity (N_0). Eq. (2) can be defined by the following parameters:

$$t = aZ - b \qquad (3)$$

$$a = \text{slope} = \frac{N_0}{C_0 U} \qquad (4)$$

$$b = \text{intercept} = \frac{1}{C_0 k_{AB}} \ln\left(\frac{C_0}{C_b} - 1\right) \qquad (5)$$

The lines of t–Z at values of $C_t/C_0 = 0.05$, 0.25, and 0.5 are shown in Fig. 6. The uncertainties of the relative parameters and BDST parameters are also listed in Table 3.

From Table 3, all the determination coefficients (R^2) adsorbed by RHC exceed 0.99, indicating that the BDST model might be applicable for the present system. However, the coefficients R^2 values of RHA are not as high as RHC. The BDST model constant can be helpful to scale up the process for other flow rates and concentration without further experimental run. These results indicate that the equation can be used to predict the adsorption performance at other operating conditions for MB adsorption by RHA and RHC.

3.3.2. Thomas model

Thomas model is another widely used model in fixed-bed performance theory. It was developed by Thomas [40] in 1944 which assumes a Langmuir isotherm for equilibrium and the adsorption is the rate driving force which obeys a second-order reversible reaction kinetics. This model is suitable for adsorption processes without axial dispersion. Meanwhile, the external and internal diffusion limitations are absent.

The expression of Thomas model is given as follows:

$$\frac{C_t}{C_0} = \frac{1}{1 + \exp((q_0 m - C_0 vt)k_{Th}/v)} \qquad (6)$$

The linearized expression of this model can be transformed into the following form for ease of calculation:

$$\ln\left(\frac{C_0}{C_t} - 1\right) = \frac{k_{Th} q_0 m}{v} - k_{Th} C_0 t \qquad (7)$$

As shown in Table 4, a good relationship between experimental and theoretical data ($R^2 < 0.8$) cannot be obtained for the MB adsorption by RHC and RHA for all breakthrough curves, even in the region below to 50% saturation.

3.3.3. Yoon–Nelson model

Yoon–Nelson model is a simple theoretical model which is originally used on the adsorption of vapors
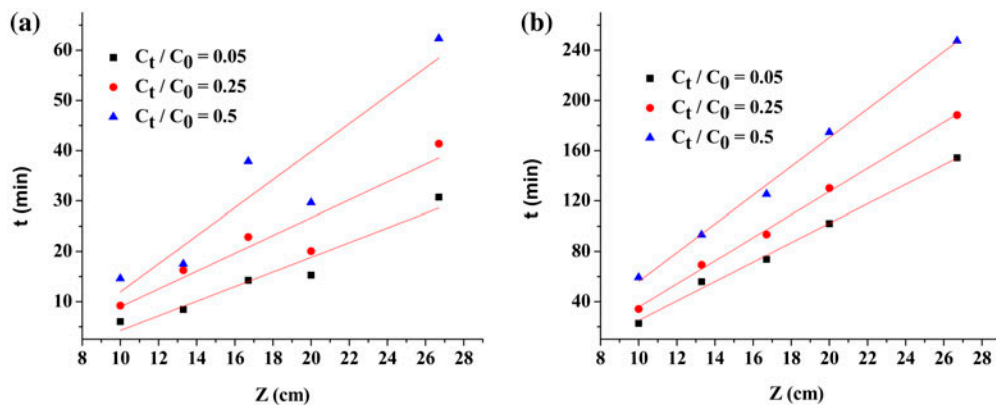
Fig. 6. Linear regression of 0.05, 0.25, 0.5 breakthrough for different bed height by (a) RHA and (b) RHC.

Table 3
Calculated constants of BDST model for the adsorption of MB using linear regression analysis ($C_0 = 20$ mg L^{-1}, $v = 10$ mL min^{-1})

C_t/C_0	0.05	0.25	0.50
RHA			
R^2	0.9257	0.8655	0.8271
N_0	227.7	276.6	435.3
k_{AB}	0.02850	0.01258	–
RHC			
R^2	0.9941	0.9967	0.9949
N_0	1,206	1,435	1,786
k_{AB}	0.005645	0.001958	–

Table 4
The correlation coefficient of Thomas model for the adsorption of MB using linear regression analysis ($C_0 = 20$ m L^{-1}, $v = 10$ mL min^{-1})

Bed heights (mm)	100	133	167	200	267
R^2 (RHA)	0.6766	0.4457	0.5739	0.5366	0.4052
R^2 (RHC)	0.7071	0.6489	0.5826	0.6967	0.6334

or gases in activated coal. It assumes that the rate of decrease in the probability of adsorption for each adsorbate molecule is proportional to the probability of adsorbate adsorption and the probability of adsorbate breakthrough on the adsorbent [41]. The Yoon–Nelson equation can be expressed as:

$$\ln\left(\frac{C_t}{C_0 - C_t}\right) = k_{YN}t - \tau k_{YN} \tag{8}$$

This model is not suitable for this study because good relationship between experimental and theoretical

data ($R^2 < 0.6$) cannot be obtained for all breakthrough curves, even in the region below 50% saturation.

The adsorption capacity (q_0) of MB on some other low-cost adsorbents collected from literature data are shown in Table 5. It is indicated that the capacity of RHC column is relatively higher than some low-cost adsorbents. However, the adsorption capacities of many adsorbents are higher than RHC in our study. Because the preparation is relatively simple and the raw material comes from agricultural wastes, RHC has a great potential for the application in wastewater treatment.

3.4. Regeneration of the column

The regeneration efficiencies by various methods are calculated and listed in Table 6. After regenerating three times, the RE decreased slightly and the RHA column showed higher RE than that of RHC column. The RE of RHA column by ethanol treatment was higher than 87%, even after three cycles. Leechart et al. [49] found that if the adsorptive dye can be eluted by acids or bases, the attachment of the dye onto the adsorbent is by ion exchange. If organic acid solvents can desorb the dye, it can be said that the adsorption of the dye onto the adsorbent is by chemisorption. Ethanol treatment resulted in the highest RE for RHA column. The effectiveness of ethanol treatment in the regeneration of MB-loaded RHA and the adsorption of the MB onto the RHA is by chemical adsorption mechanism. The regeneration efficiencies for RHC column are lower than RHA column, which may be due to the stronger forces between MB molecules and RHC.

3.5. Practical wastewater treatment

In order to study the application of RHA and RHC for the removal of dye compounds, the practical

Table 5
Bed capacity of different adsorbents for MB adsorption

Materials	Operation condition			Adsorption capacity	References
	C_0 (mg L^{-1})	Q (mL min^{-1})	Z (cm)	q_0 (mg g^{-1})	
Rice husk	50	8.2	39	6.63	[42]
Zeolite	30	2.2	15	4.36	[43]
Iron oxide-coated zeolite	30	9	16	12.5	[44]
Activated carbon	100	5	–	7.00	[45]
Bamboo charcoal	200	100	12 g	29.26	[46]
Fungal biomass	–	–	–	15.5	[47]
Chitosan-clay composite	200	5	3.6	142.31	[48]
RHA	20	10	20	5.33	This study
RHC	20	10	20	16.26	This study

Table 6
RE at different conditions

Methods	0.1 mol L^{-1} HCl		Microwave		Ethanol	
	RHA	RHC	RHA	RHC	RHA	RHC
RE% (1st cycle)	58.3	40.8	77.8	27.7	99.5	44.0
RE% (2nd cycle)	57.7	21.6	66.2	16.5	96.4	42.3
RE% (3rd cycle)	51.8	17.6	59.3	12.1	87.4	38.4

wastewater samples should be investigated. The adsorption capacity of RHA and RHC column were 5.15 and 16.0 mg g^{-1}, respectively, which have reached the capacity of 96.7 and 98.4% than that of ideal conditions. Other than MB molecules, the practical wastewater contains a great quantity of auxiliaries including various electrolytes, alkaline materials, and other compounds. The auxiliaries in the practical dye wastewater may have a competitive effect on the adsorption of MB onto adsorbents and the adsorption force may be interfered by the electrolytes. As a result, the adsorption capacity was a little lower than that of ideal conditions. However, the results showed that no significant difference was observed on the adsorption capacity, suggesting that RHC and RHA can be used to treat practical wastewater.

4. Conclusions

The rice husk/CoFe$_2$O$_4$ nanocomposite was successfully synthesized and its physicochemical properties such as BET surface area were studied. Surface area and pore size distribution of RHA and RHC indicate that RHC exhibited lower BET surface area and higher mesopore volume than that of RHA. MB adsorption by RHA and RHC were studied in fixed-bed columns. The column data were fitted by BDST, Thomas model, and Yoon–Nelson models. BDST model is the most suitable model to describe the MB adsorption by RHA and RHC. Based on the experimental results, RHC exhibits higher efficiency for MB removal from aqueous solutions in a fixed-bed column than that of RHA. Regeneration studies indicate that ethanol treatment is the most efficient method to regenerate the RHA column. Successive regeneration cycles suggest that the regenerated RHA retained high adsorption efficiency. Both RHA and RHC are effective adsorbents for the removal of dyes from practical wastewater.

Acknowledgment

Symbols

t	—	service time (min)
C_t	—	concentration of sorbate in outlet of column at time t (mg L^{-1})
C_0	—	initial sorbate concentration (mg L^{-1})
C_b	—	the concentration of adsorbate at breakthrough time (mg L^{-1})
k_{AB}	—	BDST rate constant (L mg^{-1} min^{-1})
N_0	—	adsorption capacity of the fixed-bed system (mg L^{-1})
U	—	linear flow velocity (cm min^{-1})
Q	—	flow rate (mL min^{-1})
Z	—	bed height (cm)
k_{Th}	—	Thomas rate constant (L min^{-1} mg^{-1})
q_0	—	adsorption capacity of the adsorbate–adsorbent system (mg L^{-1})
q_r	—	adsorption capacity of the regenerated column (mg g^{-1})
m	—	mass of the adsorbent in the column (g)
v	—	volumetric flow rate (L min^{-1})
k_{YN}	—	Yoon–Nelson rate constant (min^{-1})
τ	—	the time required for reach 50% adsorbate breakthrough (min)
t_b	—	breakthrough time (min)
V_b	—	breakthrough volume (mL)
T	—	temperature (K)
AC	—	activated carbon
BET	—	Brunauer, Emmet and Teller
BJH	—	Barrett–Joyner–Halenda
MB	—	methylene blue
SEM	—	scanning electron microscope
XRD	—	X-ray diffraction
RHA	—	rice husk ash
RHC	—	rice husk/CoFe$_2$O$_4$
λ	—	spectrophotometer wavelength (nm)
θ	—	XRD angle (°)
R^2	—	coefficient of determination

References

[1] R. Sanghi, P. Verma, Decolorisation of aqueous dye solutions by low-cost adsorbents: A review, Color. Technol. 129 (2013) 85–108.

[2] C. O'Neill, F.R. Hawkes, D.L. Hawkes, N.D. Lourenco, H.M. Pinheiro, W. Delee, Colour in textile effluents—Sources, measurement, discharge consents and simulation: A review, J. Chem. Technol. Biotechnol. 74 (1999) 1009–1018.

[3] V. Vadivelan, K.V. Kumar, Equilibrium, kinetics, mechanism, and process design for the sorption of methylene blue onto rice husk, J. Colloid Interface Sci. 286 (2005) 90–100.

[4] A. Rezaee, H. Masoumbaigi, R.D.C. Soltani, A.R. Khataee, S. Hashemiyan, Photocatalytic decolorization of methylene blue using immobilized ZnO nanoparticles prepared by solution combustion method, Desalin. Water Treat. 44 (2012) 174–179.

[5] R.F. Yu, H.W. Chen, W.P. Cheng, Y.J. Lin, C.L. Huang, Monitoring of ORP, pH and DO in heterogeneous Fenton oxidation using nZVI as a catalyst for the treatment of azo-dye textile wastewater, J. Taiwan Inst. Chem. Eng. 45 (2014) 947–954.

[6] C.A. Martinez-Huitle, E. Brillas, Decontamination of wastewaters containing synthetic organic dyes by electrochemical methods: A general review, Appl. Catal. B 87 (2009) 105–145.

[7] G. Masmoudi, R. Trabelsi, E. Ellouze, R.B. Amar, New treatment at source approach using combination of microfiltration and nanofiltration for dyeing effluents reuse, Int. J. Environ. Sci. Technol. 11 (2014) 1007–1016.

[8] S. Raghu, C.A. Basha, Chemical or electrochemical techniques, followed by ion exchange, for recycle of textile dye wastewater, J. Hazard. Mater. 149 (2007) 324–330.

[9] R.A. Pereira, M.F.R. Pereira, M.M. Alves, L. Pereira, Carbon based materials as novel redox mediators for dye wastewater biodegradation, Appl. Catal. B 144 (2014) 713–720.

[10] K.Y. Foo, B.H. Hameed, An overview of dye removal via activated carbon adsorption process, Desalin. Water Treat. 19 (2010) 255–274.

[11] A. Dabrowski, Adsorption—From theory to practice, Adv. Colloid Interface Sci. 93 (2001) 135–224.

[12] M.T. Uddin, M. Rukanuzzaman, M.M.R. Khan, M.A. Islam, Adsorption of methylene blue from aqueous solution by jackfruit (*Artocarpus heteropyllus*) leaf powder: A fixed-bed column study, J. Environ. Manage. 90 (2009) 3443–3450.

[13] E.N. El Qada, S.J. Allen, G.A. Walker, Adsorption of basic dyes from aqueous solution onto activated carbons, Chem. Eng. J. 135 (2008) 174–184.

[14] G.Crini, Non-conventional low-cost adsorbents for dye removal: A review, Bioresour. Technol. 97 (2006) 1061–1085.

[15] Y.F. Shen, P.T. Zhao, Q.F. Shao, Porous silica and carbon derived materials from rice husk pyrolysis char, Microporous Mesoporous Mater. 188 (2014) 46–76.

[16] P. Vassileva, A. Detcheva, I. Uzunov, S. Uzunova, Removal of metal ions from aqueous solutions using pyrolyzed rice husks: Adsorption kinetics and equilibria, Chem. Eng. Commun. 200 (2013) 1578–1599.

[17] Y. Safa, H.N. Bhatti, Kinetic and thermodynamic modeling for the removal of Direct Red-31 and Direct Orange-26 dyes from aqueous solutions by rice husk, Desalination 272 (2011) 313–322.

[18] M. Bhagiyalakshmi, L.J. Yun, R. Anuradha, H.T. Jang, Utilization of rice husk ash as silica source for the synthesis of mesoporous silicas and their application to CO_2 adsorption through TREN/TEPA grafting, J. Hazard. Mater. 175 (2010) 928–938.

[19] S. Sugashini, K.M.M.S. Begum, Adsorption and desorption studies on the performance of Fe-loaded chitosan carbonized rice husk for metal ion removal, Desalin. Water Treat. 51 (2013) 7764–7774.

[20] S. Chowdhury, P. Das Saha, Scale-up of a dye adsorption process using chemically modified rice husk: Optimization using response surface methodology, Desalin. Water Treat. 37 (2012) 331–336.

[21] R.P. Han, D.D. Ding, Y.F. Xu, W.H. Zou, Y.F. Wang, Y.F. Li, L. Zou, Use of rice husk for the adsorption of congo red from aqueous solution in column mode, Bioresour. Technol. 99 (2008) 2938–2946.

[22] D. Kalderis, D. Koutoulakis, P. Paraskeva, E. Diamadopoulos, E. Otal, J.O. del Valle, C. Fernandez-Pereira, Adsorption of polluting substances on activated carbons prepared from rice husk and sugarcane bagasse, Chem. Eng. J. 144 (2008) 42–50.

[23] Z. Razavi, N. Mirghaffari, B. Rezaei, Adsorption of crude and engine oils from water using raw rice husk, Water Sci. Technol. 69 (2014) 947–952.

[24] K.K. Senapati, C. Borgohain, P. Phukan, Synthesis of highly stable $CoFe_2O_4$ nanoparticles and their use as magnetically separable catalyst for Knoevenagel reaction in aqueous medium, J. Mol. Catal. A: Chem. 339 (2011) 24–31.

[25] Y.B. Wang, H.Y. Zhao, M.F.Q. Li, J.H. Fan, G.H. Zhao, Magnetic ordered mesoporous copper ferrite as a heterogeneous Fenton catalyst for the degradation of imidacloprid, Appl. Catal. B 147 (2014) 534–545.

[26] M. Gholinejad, B. Karimi, F. Mansouri, Synthesis and characterization of magnetic copper ferrite nanoparticles and their catalytic performance in one-pot odorless carbon–sulfur bond formation reactions, J. Mol. Catal. A: Chem. 386 (2014) 20–27.

[27] P.V. Kumar, M.P. Short, S. Yip, B. Yildiz, J.C. Grossman, High surface reactivity and water adsorption on $NiFe_2O_4$ (111) surfaces, J. Phys. Chem. C 117 (2013) 5678–5683.

[28] Y.J. Tu, C.F. You, C.K. Chang, T.S. Chan, S.H. Li, XANES evidence of molybdenum adsorption onto novel fabricated nano-magnetic $CuFe_2O_4$, Chem. Eng. J. 244 (2014) 343–349.

[29] X.G. Chen, S.S. Lv, Y. Ye, J.P. Cheng, S.H. Yin, Preparation and characterization of rice husk/ferrite composites, Chin. Chem. Lett. 21 (2010) 122–126.

[30] M.Y. Dong, Q. Lin, D. Chen, X.N. Fu, M. Wang, Q.Z. Wu, X.H. Chen, S.P. Li, Amino acid-assisted synthesis of superparamagnetic $CoFe_2O_4$ nanostructures for the selective adsorption of organic dyes, RSC Adv. 3 (2013) 11628–11633.

[31] L.H. Ai, H.Y. Huang, Z.L. Chen, X. Wei, J. Jiang, Activated carbon/$CoFe_2O_4$ composites: Facile synthesis, magnetic performance and their potential application for the removal of malachite green from water, Chem. Eng. J. 156 (2010) 243–249.

[32] X.G. Chen, S.S. Lv, S.T. Liu, P.P. Zhang, A.B. Zhang, J. Sun, Y. Ye, Adsorption of methylene blue by rice hull ash, Sep. Sci. Technol. 47 (2012) 147–156.

[33] X.G. Chen, S.S. Lv, P.P. Zhang, L. Zhang, Y. Ye, Thermal destruction of rice hull in air and nitrogen, J. Therm. Anal. Calorim. 104 (2011) 1055–1062.

[34] S.S. Lv, X.G. Chen, Y. Ye, S.H. Yin, J.P. Cheng, M.S. Xia, Rice hull/$MnFe_2O_4$ composite: Preparation, characterization and its rapid microwave-assisted COD removal for organic wastewater, J. Hazard. Mater. 171 (2009) 634–639.

[35] J. Deng, Y.S. Shao, N.Y. Gao, C.Q. Tan, S.Q. Zhou, X.H. Hu, $CoFe_2O_4$ magnetic nanoparticles as a highly active heterogeneous catalyst of oxone for the degradation of diclofenac in water, J. Hazard. Mater. 262 (2013) 836–844.

[36] A.S. Albuquerque, M.V.C. Tolentino, J.D. Ardisson, F.C.C. Moura, R. de Mendonca, W.A.A. Macedo, Nanostructured ferrites: Structural analysis and catalytic activity, Ceram. Int. 38 (2012) 2225–2231.

[37] M.J. Meng, Y.H. Feng, M. Zhang, Y. Liu, Y.J. Ji, J. Wang, Y.L. Wu, Y.S. Yan, Highly efficient adsorption of salicylic acid from aqueous solution by wollastonite-based imprinted adsorbent: A fixed-bed column study, Chem. Eng. J. 225 (2013) 331–339.

[38] K. Yaghmaeian, G. Moussavi, A. Alahabadi, Removal of amoxicillin from contaminated water using NH_4Cl-activated carbon: Continuous flow fixed-bed adsorption and catalytic ozonation regeneration, Chem. Eng. J. 236 (2014) 538–544.

[39] G.S. Bohart, E.Q. Adams, Some aspects of the behavior of charcoal with respect to chlorine, J. Am. Chem. Soc. 42 (1920) 523–544.

[40] H.C. Thomas, Heterogeneous ion exchange in a flowing system, J. Am. Chem. Soc. 66 (1944) 1664–1666.

[41] Y.H. Yoon, J.H. Nelson, Application of gas-adsorption kinetics. 1. A theoretical-model for respirator cartridge service life, Am. Ind. Hyg. Assoc. J. 45 (1984) 509–516.

[42] R.P. Han, Y.F. Wang, W.H. Yu, W.H. Zou, H. Shi, H.M. Liu, Biosorption of methylene blue from aqueous solution by rice husk in a fixed-bed column, J. Hazard. Mater. 141 (2007) 713–718.

[43] R.P. Han, Y. Wang, W.H. Zou, Y.F. Wang, H. Shi, Comparison of linear and nonlinear analysis in estimating the Thomas model parameters for methylene blue adsorption onto natural zeolite in fixed-bed column, J. Hazard. Mater. 145 (2007) 331–335.

[44] L. Zhao, W.H. Zou, L.N. Zou, X.T. He, J.Y. Song, R.P. Han, Adsorption of methylene blue and methyl orange from aqueous solution by iron oxide-coated zeolite in fixed bed column: predicted curves, Desalin. Water Treat. 22 (2010) 258–264.

[45] C. Sarici-Ozdemir, Removal of methylene blue by activated carbon prepared from waste in a fixed-bed column, Part. Sci. Technol. 32 (2014) 311–318.

[46] P. Liao, Z.M. Ismael, W. Zhang, S. Yuan, M. Tong, K. Wang, J. Bao, Adsorption of dyes from aqueous solutions by microwave modified bamboo charcoal, Chem. Eng. J. 195 (2012) 339–346.

[47] Y.Z. Fu, T. Viraraghavan, Column studies for biosorption of dyes from aqueous solutions on immobilised *Aspergillus niger* fungal biomass, Water SA 29 (2003) 465–472.

[48] M. Auta, B.H. Hameed, Chitosan-clay composite as highly effective and low-cost adsorbent for batch and fixed-bed adsorption of methylene blue, Chem. Eng. J. 237 (2014) 352–361.

[49] P. Leechart, W. Nakbanpote, P. Thiravetyan, Application of 'waste' wood-shaving bottom ash for adsorption of azo reactive dye, J. Environ. Manage. 90 (2009) 912–920.